CEAS AIDAA
3rd CEAS Air&Space Conference
21st AIDAA Congress

Steering Algorithms for Single Gimbal Control Moment Gyros in Box Configuration

Matteo Meschini and Fabio Curti
DIAEE-Department of Astronautical, Electrical and Energy Engineering, Sapienza University of Rome, e-mail: meschini.matteo@gmail.com – fabio.curti@uniroma1.it, Rome, Italy

Marco Anania
Thales Alenia Space Italia, e-mail: marco.anania@thalesaleniaspace.com, Rome, Italy

Keywords: *Control Moment Gyro Steering Law*

Abstract

A singularity problem for a single gimbal control moment gyros (SGCMGs) system in a Box configuration is analyzed. The Box configuration is affected by some singular states that cannot be escaped by using just a singularity robust inverse approach. In order to avoid this particular singular conditions two alternative steering methods are proposed, based on a real-time change of the Jacobian matrix forcing the CMGs units to exit the singular condition. Numerical simulations are presented in order to evaluate the system performances for a satellite attitude control system during prescribed attitude trajectories tracking maneuvers. The new algorithms are compared to existing steering laws and used with different null-motion methods.

1 Introduction

Control Moment Gyros (CMGs) are momentum exchange actuators, consisting of a flywheel rotating at a constant speed which the angular momentum vector is rotated by one supporting gimbal (single gimbal CMGs or SGCMGs), or two gimbals (double gimbal CMGs or DGCMGs). As a result, a torque is generated in the direction that is orthogonal to both the flywheel angular momentum and the gimbals rotation axes (Fig. 1).

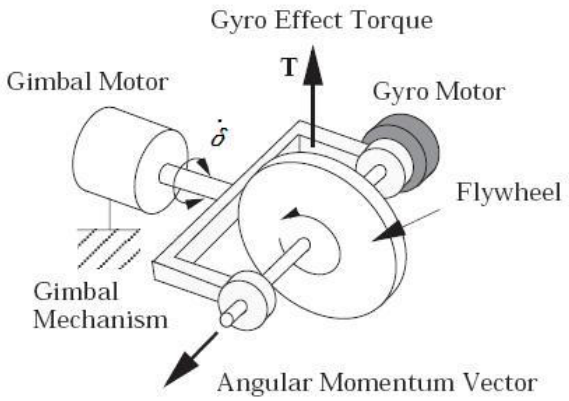

Fig. 1 Single Gimbal CMG

The main feature of the Control Moment Gyros is that they provide a high torque with a quick response with respect to the reaction wheels.

In fact, while reaction wheels can produce a maximum torque of 2 Nm, SGCMGs can reach a 5000 Nm torque capability.

The problem in using CMGs is represented by singularities that arise when a required output torque cannot be exactly provided. The control of a SGCMG cluster is based on the

inversion of the Jacobian matrix, that is a function of each CMG gimbal angle. These singular conditions come up when the classical pseudo-inverse technique is no longer usable because the matrix product between the Jacobian and his transpose results no full-rank. As a consequence the output torque cannot be given along a certain direction, denoted by the so called "singular vector".

The study of CMGs began in the 60's for the application to the Skylab's Apollo telescope mount attitude control system [1], including software studies for the actuator's steering control law.

After this studies, a double gimbal CMG system was chosen, with an approximation for the steering law Jacobian inversion.

In 1978 two independent studies by Margulies and Tokar formulate a geometric theory for singularity. Margulies introduced the gradient method null-motion for singularity avoidance, while Tokar discovered that a system with more than six SGCMG units has no internal singular states.

Based on this theory, a six SGCMG attitude control system for the MIR space station was used.

Since 1980's different approaches have been studied for the singularity avoidance of SGCMG clusters, as the *workspace reduction* [2], consisting in limiting the workspace domain of the total angular momentum or the *off-line planning*, consisting in planning the better angular momentum path before starting the maneuver.

The most studied approach is the *real-time* control, which consists in introducing a mathematical element for avoiding singularity in the Jacobian inversion.

Presently DGCMGs, which have less singularity problems, have been used on the ISS. Moreover these devices are largely studied for the attitude control of satellites thanks to the capability of constructing CMGs of small size and weight [3,4].

This work focus on the SGCMGs *real-time* control approach for a satellite attitude control system of 4 SGCMG units, aiming to analyze the behavior of two proposed steering algorithms, compared to already existing laws.

A particular configuration called Box is considered.

In order to evaluate numerical results a satellite attitude control system have been simulated, performing prescribed attitude trajectories tracking maneuvers.

The required maneuver performances are obtainable only by using CMGs actuators because of S/C high rotation rates and accelerations.

2 Mathematical Modeling

In this section the SGCMGs' (simply called CMGs by now) control theory will be described, introducing the singularity problem.

First of all, we can define the rotational motion equations of the S/C assuming it as a rigid body. Including momentum exchange actuators the equation is simply given by:

$$J\dot{\boldsymbol{\omega}} + \dot{\mathbf{h}} + \boldsymbol{\omega} \times \left(J\boldsymbol{\omega} + \mathbf{h} \right) = \mathbf{T}_{EXT} \qquad (1)$$

Where J is the S/C inertia matrix, including the actuators inertia, $\mathbf{h}$ is the CMGs actuators total angular momentum expressed in the S/C body fixed axes, the vector $\boldsymbol{\omega} = \left(\boldsymbol{\omega}_x, \boldsymbol{\omega}_y, \boldsymbol{\omega}_z \right)$ is the S/C angular velocity, and $\mathbf{T}_{EXT}$ represents the external torques.

Introducing the actuators control torque $\boldsymbol{\tau}$ we can write the Eq. (1) as a system of two equations:

$$J\dot{\boldsymbol{\omega}} + \boldsymbol{\omega} \times \left(J\boldsymbol{\omega} + \mathbf{h} \right) = \boldsymbol{\tau} + \mathbf{T}_{EXT} \qquad (2)$$

$$\dot{\mathbf{h}} = -\boldsymbol{\tau} \qquad (3)$$

The control torque $\boldsymbol{\tau}$ represents the torque given by the CMGs actuators in order to perform an assigned attitude maneuver.

We can define the CMGs total angular momentum as the sum of each unit momentum

vector, and it can be expressed as:

$$\mathbf{h} = \sum_{i=1}^{n} \mathbf{h}_i(\delta_i) \qquad (4)$$

Where $\mathbf{h}_i$ is the angular vector of the *i*-th unit, function of the gimbal angle, δ_i is the gimbal angle of the *i*-th unit representing the orientation of each unit and *n* is the actuators' units number.

To express the time derivative of Eq. (4) in order to resolve the Eq. (3) we must consider the dependence of the angular momentum vector by the gimbal angles, obtaining

$$\dot{\mathbf{h}} = \sum_{i=1}^{n} \frac{\partial \mathbf{h}_i}{\partial \delta_i} \frac{\partial \delta_i}{\partial t} = C\dot{\boldsymbol{\delta}} \qquad (5)$$

Where the *C* matrix is the system Jacobian, defined as:

$$C = \left[\frac{\partial \mathbf{h}_1}{\partial \delta_1}, \frac{\partial \mathbf{h}_2}{\partial \delta_2}, \frac{\partial \mathbf{h}_3}{\partial \delta_3}, \ldots, \frac{\partial \mathbf{h}_n}{\partial \delta_n} \right] \qquad (7)$$

And $\dot{\boldsymbol{\delta}}$ is the gimbal rates vector $\dot{\boldsymbol{\delta}} = \left[\dot{\delta}_1, \dot{\delta}_2, \dot{\delta}_3, \ldots, \dot{\delta}_n \right]^T$.

The Jacobian *C* is a $3 \times n$ dimensional matrix, and each column represents the output torque versor of the *i*-th unit, multiplied for the angular momentum module of a single unit.

To invert Eq. (5), since for redundant systems with $n>3$ (or if $n<3$) *C* is a rectangular matrix, the inversion can be made using the well known Moore-Penrose pseudoinverse (PSI), obtaining:

$$\dot{\boldsymbol{\delta}} = C^{\#}\dot{\mathbf{h}} = C^T \left[CC^T \right]^{-1} \dot{\mathbf{h}} \qquad (8)$$

Where $C^{\#}$ indicates the Jacobian matrix inverse. Equation (8) gives an exact, minimum norm, solution of $\dot{\boldsymbol{\delta}}$. On the other hand, the PSI solution exists only if CC^T is full rank. In fact, if $\det\left(CC^T\right) = 0$ the inversion in Eq. (8) is not possible and the system is in a singular state. For each singularity state a vector $\mathbf{u}$ can be defined as the *singular vector*, along which the system cannot provide torque.

A *real-time* steering control approach tries to solve this problem modifying Eq. (8) in order to give always a solution of $\dot{\boldsymbol{\delta}}$, despite the introduction of a little error while the system pass through a singular state.

2.1 The Box Configuration

The actuators cluster analyzed in this work is the so called Box configuration, that can be recognized also as a Roof type M(2,2) with orthogonal planes or a Pyramid type with a skew angle of 90 deg.

It consists of 4 SGCMGs divided in two pairs of units. Each pair has the same gimbal axis direction and the output torque lies on a plane (Fig. 2).

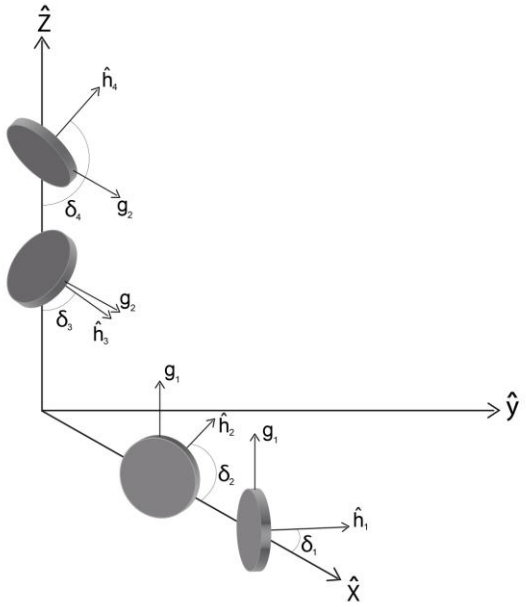

Fig. 2 Box configuration scheme

For the simulations the first units pair (CMGs 1&2) has the gimbal axis $\mathbf{g}_1$ along the body $\hat{\mathbf{z}}$ axis (Yaw axis), the gimbal angles δ_1 and δ_2 are measured starting from the $\hat{\mathbf{x}}$ axis and the generated torque lies on the *xy* plane.

The second pair (CMGs 3&4) has the gimbal axis $\mathbf{g}_2$ along the body $\hat{\mathbf{x}}$ axis (Roll axis), the gimbal angles δ_3 and δ_4 are measured starting from the $-\hat{\mathbf{z}}$ axis and the torque is given on the *yz* plane. The combination of the two pairs allow to generate a torque vector in a 3 dimensional space.

It can be now defined the total angular momentum as:

$$\mathbf{h} = H\begin{bmatrix} \cos\delta_1 + \cos\delta_2 \\ \sin\delta_1 + \sin\delta_2 + \sin\delta_3 + \sin\delta_4 \\ -\cos\delta_3 - \cos\delta_4 \end{bmatrix} \qquad (9)$$

Where H is the constant angular momentum value of each unit. The Jacobian will be:

$$C = H\begin{bmatrix} -\mathrm{s}\delta_1 & -\mathrm{s}\delta_2 & 0 & 0 \\ \mathrm{c}\delta_1 & \mathrm{c}\delta_2 & \mathrm{c}\delta_3 & \mathrm{c}\delta_4 \\ 0 & 0 & \mathrm{s}\delta_3 & \mathrm{s}\delta_4 \end{bmatrix} \qquad (10)$$

Where $\mathrm{s}\delta_i = \sin\delta_i$ and $\mathrm{c}\delta_i = \cos\delta_i$.

The singular states for the Box configuration are defined by the following angles conditions:

- $\delta_1 = \delta_2, \delta_3 = \delta_4$
- $\delta_1 = \delta_2 + \pi, \delta_3 = \delta_4$
- $\delta_1 = \delta_2, \delta_3 = \delta_4 + \pi$
- $\delta_1 = \delta_2 + \pi, \delta_3 = \delta_4 + \pi$
- $\delta_1 = \delta_2 = k\pi$
- $\delta_1 = k\pi, \delta_2 = \delta_1 + \pi$
- $\delta_3 = \delta_4 = k\pi$
- $\delta_3 = k\pi, \delta_4 = \delta_3 + \pi$

(11)

Where k=0, 1.

The comparison with the Pyramid type configuration shows that in case of failure of one CMG, the Box configuration assure the largest singularity free internal workspace, allowing a simpler torque generation with respect to a conventional Pyramid configuration [5].

Moreover, as visible analyzing Eq. (9), the Box configuration angular momentum workspace is near-ellipsoidal with a momentum capacity of $4H$ along the pitch axis and a capacity of $2H$ along the roll and yaw axes, in order to improve maneuvering performances for pitch rotations, while for a Pyramid configuration it is possible to obtain a near spherical workspace.

3 Conventional Real-time Steering Laws

Most of the *real-time* steering methods are based on the solution of a mixed, two-norm and least-squares minimization problem:

$$\min_{\dot{\boldsymbol{\delta}}}\left\{\left(C\dot{\boldsymbol{\delta}} - \mathbf{T}\right)^T P\left(C\dot{\boldsymbol{\delta}} - \mathbf{T}\right) + \dot{\boldsymbol{\delta}}^T Q\dot{\boldsymbol{\delta}}\right\} \qquad (12)$$

Subject to $C\dot{\boldsymbol{\delta}} = \mathbf{T}$ (13)

Where $\mathbf{T}$ is the required torque and P and Q are positive definite square matrices. This time the inversion of the Jacobian can be found as:

$$C^{\#} = WC^T\left[CWC^T + V\right]^{-1} \qquad (14)$$

Where W=Q^{-1} and V=P^{-1}.

The first Singularity Robust Inverse (SRI) steering method, proposed by Nakamura and Hanafusa [6], identified W and V as $W = I_{n\times n}$ and $V = \lambda I_{3\times 3}$, where λ is a properly chosen positive scalar needed to avoid the singular state. As a result, Eq. (14) becomes:

$$C^{\#} = C^T\left[CC^T + \lambda I_{3\times 3}\right]^{-1} \qquad (15)$$

The scalar λ is often selected as:

$$\lambda = \lambda_0 \exp\left[-\mu \det\left(CC^T\right)\right] \qquad (16)$$

Where λ and μ are positive scalars to be properly selected. It can be emphasized that in a

singular state $\det\left(CC^T\right)=0$ and λ tends to λ_0, permitting the existence of Eq. (15).

Though the SRI method is effective for the most of internal singularities, when the required torque lies along the singular vector the solution $\dot{\boldsymbol{\delta}}$ is a null vector, and the system cannot escape the singular state.

In order to avoid this problem Wie, Bailey and Heiberg [7] modified the SRI introducing a time dependent matrix able to pass through such a singular state.

This method, called Perturbed Singularity Robust inverse (PSR) by now, is defined by the two matrices $W=I_{n\times n}$ and $V=\lambda E$:

$$C^{\#}=C^T\left[CC^T+\lambda E\right]^{-1} \qquad (17)$$

Where

$$E=\begin{bmatrix}1 & \varepsilon_3 & \varepsilon_2\\ \varepsilon_3 & 1 & \varepsilon_1\\ \varepsilon_2 & \varepsilon_1 & 1\end{bmatrix} \qquad (18)$$

and

$$\varepsilon_i=\varepsilon_0\sin\left(\omega t+\varphi_i\right) \qquad (19)$$

Where t is the time and the amplitude ε_0, the frequency ω and the phases φ_i need to be properly selected.

All the SR based methods act modifying the output torque permitting to quit the singular state while introducing an error.

3.1 Null Motion

In addition to the solution given by the Jacobian inversion another component can be added to improve the singularity avoidance for redundant systems. This element uses the null space of the Jacobian in order to do not produce torque, while adding a proper amount of null motion $\dot{\boldsymbol{\delta}}_N$ that can be used to allow the system to steer away from passable singularities or to maintain the CMGs near a desired position.

The null motion component is defined as:

$$\dot{\boldsymbol{\delta}}_N=\left[I-C^{\#}C\right]\cdot\mathbf{d} \qquad (20)$$

Where $\mathbf{d}$ is a vector representing the amount of null motion for each unit. In every non singular state it is assured that $C\dot{\boldsymbol{\delta}}_N=0$.

Depending on the selection of $\mathbf{d}$ two principal null motion types can be defined.

The *gradient method* [2] defines $\mathbf{d}$ as a gradient of a certain function $f\left(\boldsymbol{\delta}\right)$ permitting its maximization. The function $f\left(\boldsymbol{\delta}\right)$ can be selected as a measure of singularity, such as $f\left(\boldsymbol{\delta}\right)=\det\left(CC^T\right)$.

Another type of null motion, called *preferred gimbal angles* [8], makes possible to maintain the units around a fixed position $\boldsymbol{\delta}_0$, making possible the introduction gimbal rotations constraints and increasing the reliability of the system.

4 Saturation Singularities Escape

The PSR is a steering control law effective for almost every so called internal singularities, but for the saturation singular states can present problems. In fact, when the system reach the angular momentum saturation, though the conventional steering laws produce the CMGs rotation, the system remains in a saturation state preventing actuators desaturation.

For the Box configuration this problem appears when one or more pairs of CMGs get the same orientation resulting aligned.

In this case 2 or 4 rows of $C^{\#}$ are equals and the generated rotation rates $\dot{\delta}_i$ have the same values for each pair of units, preventing the separation.

This causes the permanency in a singular state, or the increase of chances to ran into singularities.

This problem related to saturation singularities was faced by Wie in 2005 [9], proposing a modification of the PSR. He

proposed to change the W matrix of Eq. (14) in a near diagonal matrix obtaining:

$$C^{\#} = WC^{T}\left[CWC^{T} + \lambda E\right]^{-1} \qquad (21)$$

With

$$W = \begin{bmatrix} w_1 & \gamma & \gamma & \gamma \\ \gamma & w_2 & \gamma & \gamma \\ \gamma & \gamma & w_3 & \gamma \\ \gamma & \gamma & \gamma & w_4 \end{bmatrix} \qquad (22)$$

Where the diagonal elements w_i are positive scalars and $\gamma \cong 0$. The λE term is the same as the one used for PSR.

The purpose of the W matrix is to change the gimbal rates of the aligned units in order to separate them while generating near the same PSR torque error. This method has been called *Off-Diagonal SRI* (o-DSR).

Another solution has been proposed by Heiberg in 2011 [10], providing singularity avoidance using virtual array rotations. This steering logic is based on the evaluation of the determinant of CC^{T}: If its value is less than a certain threshold the Jacobian C is recalculated with a virtual gimbal angle displacement, in order to bypass the singular state and generate a torque affected by an error caused by the virtual displacements. The Jacobian evaluation and recalculation is done while the determinant reaches the threshold value.

This method allow to pass even the saturation singularities and in addiction, with respect to the o-DSR, it needs a routine with a decision block to calculate the gimbal rates $\dot{\boldsymbol{\delta}}$.

5 Proposed Steering Control Algorithms

The two proposed steering control logics are based on the PSR method together with a Jacobian change during the alignment of any units pair.

The first method (called PA1 by now) includes an evaluation of the angle between each pair of units and since the saturation singularities are caused by alignment of one or two couples of CMGs, a change of Jacobian is made in order to separate them.

If the relative displacement become less than a threshold value, the Jacobian is changed removing the column associated to the CMG that is needed to stop.

So the non stopped unit become steered like the system has only 3 units (or 2) while the stopped one is not considered in the PSR control law until the relative angle between them exceeds the threshold value.

The logic can be reassumed by the following table:

Tab. 1 PA1 logic

Angles conditions	Jacobian suppressed columns
$\lvert\delta_1-\delta_2\rvert > \Delta\delta_{\lim}$ $\lvert\delta_3-\delta_4\rvert > \Delta\delta_{\lim}$	None
$\lvert\delta_1-\delta_2\rvert \le \Delta\delta_{\lim}$ $\lvert\delta_3-\delta_4\rvert > \Delta\delta_{\lim}$	2nd
$\lvert\delta_1-\delta_2\rvert > \Delta\delta_{\lim}$ $\lvert\delta_3-\delta_4\rvert \le \Delta\delta_{\lim}$	4th
$\lvert\delta_1-\delta_2\rvert \le \Delta\delta_{\lim}$ $\lvert\delta_3-\delta_4\rvert \le \Delta\delta_{\lim}$	2nd and 4th

Where $\Delta\delta_{\lim}$ is the threshold value for the units couples relative displacement.

In Fig. 3 the system behavior is shown: On the left the CMGs couple is in an aligned condition, producing torque on the xy plane, while on the right is shown the response given through the new steering logic.

On the right is also possible to observe that the total torque is near the same as the one given by the PSR method, thanks to the increased rate for the non stopped CMG.

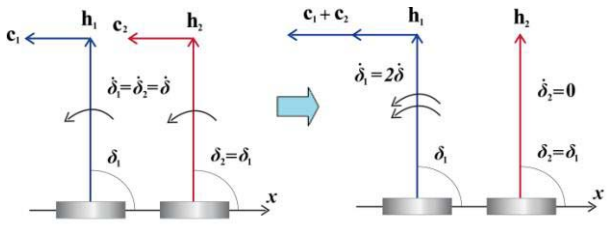

Fig. 3 PA1 Jacobian change effect

The second proposed steering algorithm (called PA2 by now) is based on the first one. The Jacobian change is made in the same way as described before, but a manipulation of the gimbal rates is made. In order to increase the separation velocity, instead of move one CMG stopping the other, a velocity component is added to both the units in opposites directions.

The gimbal rates manipulation can be schematized as follows:

Tab. 2 PA2 rates manipulation

PA1 resultant gimbal rates	New gimbal rates
$\dot{\boldsymbol{\delta}}=\left[\dot{\delta}_1,0,\dot{\delta}_3,\dot{\delta}_4\right]$	$\dot{\boldsymbol{\delta}}_{NEW}=\left[\frac{3}{2}\cdot\dot{\delta}_1,-\frac{1}{2}\cdot\dot{\delta}_1,\dot{\delta}_3,\dot{\delta}_4\right]$
$\dot{\boldsymbol{\delta}}=\left[\dot{\delta}_1,\dot{\delta}_2,\dot{\delta}_3,0\right]$	$\dot{\boldsymbol{\delta}}_{NEW}=\left[\dot{\delta}_1,\dot{\delta}_2,\frac{3}{2}\cdot\dot{\delta}_3,-\frac{1}{2}\cdot\dot{\delta}_3\right]$
$\dot{\boldsymbol{\delta}}=\left[\dot{\delta}_1,0,\dot{\delta}_3,0\right]$	$\dot{\boldsymbol{\delta}}_{NEW}=\left[\frac{3}{2}\cdot\dot{\delta}_1,-\frac{1}{2}\cdot\dot{\delta}_1,\frac{3}{2}\cdot\dot{\delta}_3,-\frac{1}{2}\cdot\dot{\delta}_3\right]$

For example, being $\dot{\boldsymbol{\delta}}=\left[\dot{\delta}_1,0,\dot{\delta}_3,\dot{\delta}_4\right]$ the gimbal rate vector obtained by the first method, the rate vector for the second method can be obtained as $\dot{\boldsymbol{\delta}}_{NEW}=\left[3/2\cdot\dot{\delta}_1,-1/2\cdot\dot{\delta}_1,\dot{\delta}_3,\dot{\delta}_4\right]$.

So the behavior of CMGs 1&2 can be shown in Fig. 4.

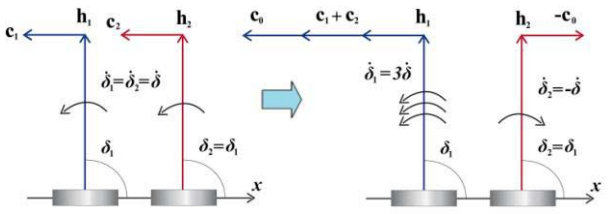

Fig. 4 PA2 solution

And the separation velocity will be $\left|\Delta\dot{\delta}_{1-2}\right|=2\cdot\dot{\delta}_1$, that is the double of the one obtained by the first method. The resultant torque is the same as the one given by the first proposed logic.

5.1 Numerical Example

Consider now a Box configuration in a saturation singularity corresponding to a gimbal angle vector $\boldsymbol{\delta}=\left[70,70,150,150\right]\text{deg}$.

Choosing the angular momentum of each unit as H=1 *Nms*, the Jacobian defined by Eq. (10) becomes:

$$C=\begin{bmatrix}-0.940 & -0.940 & 0 & 0\\ 0.342 & 0.342 & -0.866 & -0.866\\ 0 & 0 & 0.500 & 0.500\end{bmatrix} \quad (23)$$

To calculate the expressions defined by Eq. (16), Eq. (18) and Eq. (19) the following values are chosen: $\lambda_0=0.01$, $\mu=10$, $\varepsilon_0=0.01$, $\omega=\pi/2$, $\boldsymbol{\varphi}=\left[0,\pi/2,\pi\right]$ and t=15 *s*. The W matrix for the o-DSR is selected as W=diag(1,2,3,4).

For this example the desired torque will be $\mathbf{T}=\dot{\mathbf{h}}=\left[-1,0,0\right]^T\ Nm$.

The PSR steering law defined by Eq. (17) provides:

$$C^{\#}=\begin{bmatrix}-0.511 & 0.049 & 0.083\\ -0.511 & 0.049 & 0.083\\ 0.151 & -0.417 & 0.272\\ 0.151 & -0.417 & 0.272\end{bmatrix} \quad (24)$$

And the gimbal rate vector $\dot{\boldsymbol{\delta}}=C^{\#}\mathbf{T}$ becomes:

$$\dot{\boldsymbol{\delta}}_{PSR}=\left[0.51,\ 0.51,\ 0.15,\ 0.15\right]rad/s \quad (25)$$

As can be seen, the CMGs 1&2 gimbal rates are equals, as well as the CMGs 3&4 ones, preventing the singularity escape.

The torque $\mathbf{T}=C\dot{\boldsymbol{\delta}}$ given by PSR is:

$$\mathbf{T}_{PSR}=\left[-0.9611,\ 0.0883,\ 0.1510\right]Nm \quad (26)$$

The o-DSR described by Eq. (21) gives the following rate solution and torque:

$$\dot{\boldsymbol{\delta}}_{o-DSR} = \left[0.34,\ 0.68,\ 0.13,\ 0.17\right] rad/s \qquad (27)$$

$$\mathbf{T}_{o-DSR} = \left[-0.9632,\ 0.0875,\ 0.1519\right] Nm \qquad (28)$$

For the method proposed by Heiberg, choosing a virtual displacement of 1° for the 2nd and 3rd CMG units we obtain the Jacobian as:

$$C = \begin{bmatrix} -0.940 & -0.946 & 0 & 0 \\ 0.342 & 0.326 & -0.866 & -0.875 \\ 0 & 0 & 0.500 & 0.485 \end{bmatrix} \qquad (29)$$

And the rate vector and output torque are:

$$\dot{\boldsymbol{\delta}}_{HEI} = \left[-3.58,\ 4.62,\ -7.73,\ 7.97\right] rad/s \qquad (30)$$

$$\mathbf{T}_{HEI} = \left[-0.9731,\ 0.1445,\ 0.1211\right] Nm \qquad (31)$$

For the first proposed steering algorithm (PA1) in the new Jacobian the 2nd and 4th columns are suppressed in order to stop CMGs 2&4 and permit the couples separation, obtaining:

$$C = \begin{bmatrix} -0.940 & 0 \\ 0.342 & -0.866 \\ 0 & 0.500 \end{bmatrix} \qquad (32)$$

So the rate vector and output torque become:

$$\dot{\boldsymbol{\delta}}_{PA1} = \left[1.017,\ 0,\ 0.299,\ 0\right] rad/s \qquad (33)$$

$$\mathbf{T}_{PA1} = \left[-0.9555,\ 0.0891,\ 0.1493\right] Nm \qquad (34)$$

The second proposed logic (PA2) provides the following rate vector and torque:

$$\dot{\boldsymbol{\delta}}_{PA2} = \left[1.53,\ -0.51,\ 0.45,\ -0.15\right] rad/s \qquad (35)$$

$$\mathbf{T}_{PA2} = \left[-0.9555,\ 0.0891,\ 0.1493\right] Nm \qquad (36)$$

The results show that the output torque during the singular state presents comparable errors. The main difference between the different steering laws is represented by the gimbal rates. In fact the separation velocity for CMGs 1&2 are: $\Delta\dot{\delta}_{o-DSR} = \left|\dot{\delta}_1 - \dot{\delta}_2\right| = 0.34\ rad/s$ $\Delta\dot{\delta}_{HEI} = 8.20\ rad/s$, $\Delta\dot{\delta}_{PA1} = 1.017\ rad/s$ and $\Delta\dot{\delta}_{PA2} = 2.034\ rad/s$.

Usually a real gimbal motor can provide gimbal rates often limited to $1 \div 2\ rad/s$ and accelerations limited to few rad/s^2 and in case of gimbal rates saturation, a proportional scaling for all the CMGs rates is made, in order to maintain the output torque along the desired direction even if decreased in value.

So even if in an ideal system the Heiberg steering logic would be preferable with respect to the others because of its higher separation velocity, probably the high rates shown by Eq. (30) would be limited by the motor constraints, affecting the output torque more than the others methods.

6 Simulation Results

In order to evaluate the effectiveness of the presented steering logics a large quantity of simulations have been carried out simulating a typical Earth observation mission in a sun-synchronous orbit. During simulations ideal sensors and ideal gimbal motors have been considered, together with a rate saturation to $\dot{\delta}_{\lim} = \pm 1\ rad/s$ and an acceleration limit of $\ddot{\delta}_{\lim} = \pm 1\ rad/s^2$. The gravity gradient torque has been introduced as external torque.

To calculate the torque needed by CMGs for the prescribed attitude trajectories tracking maneuvers a PID controller was used, together with a feedback-linearization component and a

feed-forward control torque based on the reference S/C accelerations, developed as:

$$\boldsymbol{\tau} = -K_P\mathbf{e} - K_D\left(\boldsymbol{\omega} - \boldsymbol{\omega}_r\right) - K_I\int \mathbf{e}\,dt + \\ + J\dot{\boldsymbol{\omega}}_r + \boldsymbol{\omega}\times J\boldsymbol{\omega} + \boldsymbol{\omega}\times\mathbf{h} \qquad (37)$$

Where the torque $\boldsymbol{\tau}$ has been defined in Eq. (3), K_P, K_D and K_I are diagonal and definite positive matrices, $\boldsymbol{\omega}$ is the measured angular rate of the S/C, $\boldsymbol{\omega}_r$ is the reference S/C rate, $\mathbf{h}$ is the actuators angular momentum vector, $\mathbf{e}$ is the quaternion error vector and J is the S/C inertial matrix, that for the analyzed satellite has been taken:

$$J = \begin{bmatrix} 7500 & 375 & 750 \\ 375 & 11250 & 150 \\ 750 & 150 & 9000 \end{bmatrix} kg\cdot m^2 \qquad (38)$$

The following simulation results are referred to a 30 deg pitch-axis reorientation maneuver, depicted in Fig. 5.

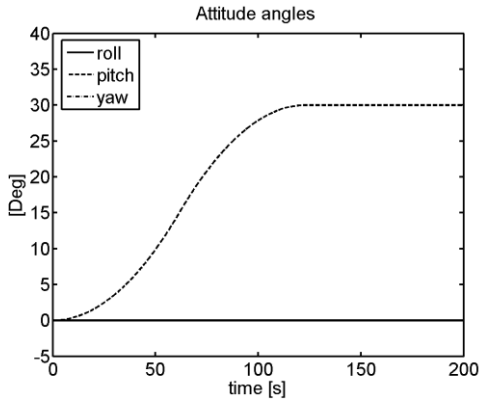

Fig. 5 Pitch-axis reorientation maneuver

For this simulation it will be considered a worst case, starting from a singular state that cannot be escaped by the SRI or PSR as described before.

The set of the initial gimbal angles is chosen as $\boldsymbol{\delta}_0 = [80,80,260,260]$ deg and the angular momentum of each CMG is assumed as H=30 *Nms*. The values of λ, E and W have been already defined in the previous paragraph. The angle threshold value for PA1 and PA2 has been set to $\Delta\delta_{\text{lim}} = 0.1$ deg.

In Fig. 6 the attitude errors obtained by each steering law are showed, and as can be seen, the error values are well comparable. At the beginning of the maneuver the escape from the initial singularity produces a larger error for the PA1, while for the o-DSR it becomes very small.

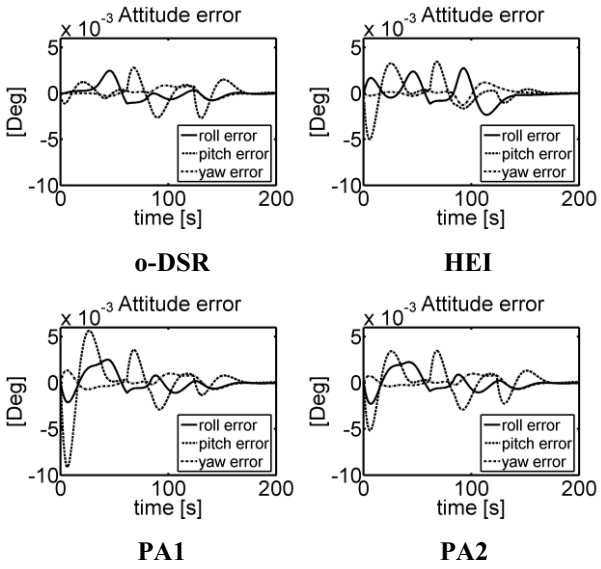

Fig. 6 Attitude angles errors

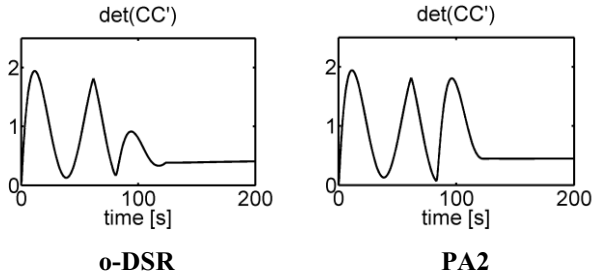

Fig. 7 det(CC^T) time histories

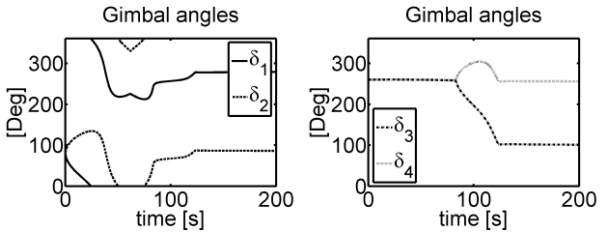

Fig. 8 CMG gimbal angles time history for PA2

In Fig. 7 the determinant time histories for the o-DSR and PA2 are represented, showing an higher average value for PA2, whereas in Fig. 8

it is possible to see the gimbal angles time history of each units couple for the PA2 (CMGs 1&2 on the left and 3&4 on the right)

The results for the PA1 are very similar to the PA2 ones and will not be shown.

To further evaluate the effectiveness of PA1 and PA2, singularity escape simulations have been carried out starting from all type of singular states related to the Box configuration.

Moreover an instrument scanning maneuver has been analyzed, using the two different methods for null motion, of which the results are not shown here. Though the main features revealed by simulations are the meeting of the attitude errors with the scanning phase errors constraints (errors < 3 mdeg) and the possibility to introduce mechanical constraints to the gimbals rotation using a preferred gimbal angles null motion, simplifying the electrical interfaces and increasing the system reliability.

7 Conclusion

Two new steering logics has been proposed for a SGCMG cluster in a Box configuration based on the PSR steering law, together with a real-time Jacobian change made in order to escape saturation singularities, non escapable by the simple PSR.

PA1 and PA2 separation velocity for the aligned units is faster than the o-DSR one, whereas the new laws do not need a routine block with respect to the Heiberg logic.

The test with different null motions has demonstrated that a gradient method can avoid certain type of singularity, while the preferred gimbal angles method makes possible the introduction of mechanical constraints to the gimbal rotations, simplifying the electrical interface and increasing reliability.

References

[1] Chubb W. B. and Seltzer S. M., "Skylab Attitude and Pointing Control System," NASA TN D-6068, 1971.

[2] Kurokawa H., "A Geometric Study of Single Gimbal Control Moment Gyros – Singularity Problems and Steering Law," Ph.D. Dissertation, Aeronautics and Astronautics, Univ. Tokyo, Japan, 1997.

[3] Lappas V. J., Steyn W. H. and Underwood C. I., "Attitude Control for Small Satellites using Control Moment Gyros," *Acta Astronautica*, Vol. 51, No. 1-9, 2002, pp. 101-111.

[4] Gersh J. and Peck M. A., "Violet: A High-Agility Nanosatellite for Demonstrating Small Control-Moment Gyroscope Prototypes and Steering Laws," *AIAA Guidance, Navigation, and Control Conference*, Chicago, IL, 2009.

[5] Sands T. A., Kim J. J. and Agrawal B., "2H Singularity-Free Momentum Generation with Non-Redundant Single Gimbaled Control Moment Gyroscopes," *IEEE Conference on Decision & Control*, San Diego, CA, 2006, pp. 1551-1556.

[6] Nakamura Y. and Hanafusa H., "Inverse Kinematic Solutions with Singularity Robustness for Robot Manipulator Control," *Journal of Dynamic Systems, Measurement, and Control*, Vol. 108, 1986, pp. 163-171.

[7] Wie B., Bailey D. and Heiberg C. J., "Singularity Robust Steering Logic for Redundant Single-Gimbal Control Moment Gyros," *Journal of Guidance, Control, and Dynamics*, Vol. 24, No. 5, 2001, pp. 865-872.

[8] Vadali S. R., Oh H. S. and Walker S. R., "Preferred Gimbal Angles for Single Gimbal Control Moment Gyros," *Journal of Guidance, Control, and Dynamics*, Vol. 13, No. 6, 1990, pp. 1090-1095.

[9] Wie B., "Singularity Escape/Avoidance Steering Logic for Control Moment Gyro Systems," U.S. Patent 6,917,862 B2, 12 July 2005.

[10] Heiberg C. J., "Singularity Escape and Avoidance using a Virtual Array Rotation," U.S. Patent 7,904,214 B2, 8 March 2011.